EAI Endorsed Transactions
on Energy Web
Research Article EAI.EU

Security Enhancement in Power System Using FACTS Devices and Atom Search Optimization Algorithm

A Amarendra[1,*], L Ravi Srinivas[2] and R Srinivasa Rao[3]

[1]Associate Professor, Department of Electrical & Electronics Engineering, Gudlavalleru Engineering College, Andhra Pradesh, India.
[2]Professor, Department of Electrical and Electronics Engineering, Gudlavalleru Engineering College, A.P., India. lravisrinivas@gmail.com
[3]Professor, Department of Electrical and Electronics Engineering, University College of Engineering, Kakinada, JNTU Kakinada, India. srinivas.jntueee@gmail.com

Abstract

In power systems, control, system operations are an important and difficult task by enhancing the power systems' security. An enhancement of the security system is done by the optimal location selection of the Flexible Alternating Current Transmission System (FACTS) devices, for instance, Unified Power Flow Controller (UPFC), Thyristor-Controlled Series Capacitor (TCSC), Interlink Power Flow Controller (IPFC), and Static VAR Compensator (SVC). Therefore, the Atom Search Algorithm (ASO) is utilized to compute the precise optimal placement of the FACTS device. FACTS devices must be in the correct location on the power system to improve system safety. The performances are evaluated by severity index, Line Overload Sensitivity Index (LOSI), voltage, voltage deviation,, power loss, fitness function, and the fuel cost with the IEEE 30, IEEE 118, and IEEE 300 bus system. To validate the proposed methodology, it is contrasted with the conventional techniques like Dragonfly Algorithm (DA), Whale Optimization Algorithm (WOA), Jaya, Flower Pollination Algorithm (FPA), Grey Wolf Algorithm (GWA), and the Jaya Flower Pollination (JA-FPA) systems.

Keywords: FACTS devices, optimization, security enhancement, stability, reliability, optimal power flow, constraints, location, atom search algorithm, and severity index.

Received on 17 January 2021, accepted on 10 April 2021, published on 16 April 2021

doi: 10.4108/eai.16-4-2021.169335

*Corresponding author. Email: amarendra@gecgudlavallerumic.in

1. Introduction

In the power networks, the complex systems increase because of dynamic load variations and load demand increase that surely affects the transmission lines. In these conditions, the power system may affect underloaded or overloaded conditions [1, 27]. These underloaded and overloaded conditions are failed to maintain the proper security concern in the power system. The power system security is an essential task towards maintaining the system firmness and authenticity conditions [2]. The stable conditions are maintained by reducing or maintaining the overload and underload scenarios in the power system. The system's security may collapse due to bus voltage violations, system variation conditions, and line overloading conditions. Therefore, dynamic safety analysis is important due to the system's constantly changing operating conditions [3]. Risk-Based Security Constrained Optimal Power Flow (RBOPF) is considered the system to manage the power system's security. The RBOPF should be solved for enabling power system security improvement. To improve security and stable operation in the power system, the power flow [4, 26].

Optimal power flow can be solved by various FACTS techniques and devices, which certainly allow safety restrictions in the power system. System security is guaranteed by the optimal placement of the FACTS device in the system, for example, SVC, TCSC [6], Thyristor-Controlled Phase-Shifting Transformer (TCPST), Static Synchronous Compensator (STATCOM) [5], UPFC [7] Thyristor-Controlled Voltage Regulator

(TCVR), and IPFC [8]. The FACTS devices should provide the highest advantage to power networks for maintaining stability and security constraints. In the power system, to maintain stability and security constraints, FACTS device placement is an essential task which high complex system [9]. The FACTS devices are located in the system by checking objective functions. Once they met their objective functions and constraints limits [10, 25], the FACTS device will be placed in the power system, which completely enhances security and stability problems [29-34].

The FACTS device placement is achieved using four methods: hybrid methods, meta-heuristic methods, conventional optimization methods, arithmetic programming, and analytic methods. The meta-heuristic methods are the well-established method to achieve the best results in the FACTS device placement and location in the power system [35-39]. The FACTS device's optimal placement is achieved considering safety restrictions [11, 28], static constraints, inequality, dynamic constraints, and nonequality constraints in the power system. The constraints are important in security enhancement, such as demand limits, power flow equations, power loss equation, transmission line thermal limits, FACTS devices ratings, reactive power, active power [12], bus voltage, and power balance equations. Many numerous meta-heuristic approaches are utilized to compute the FACTS devices, optimal allocation of in the power system to enhance security, and stability conditions, such as Particle Swarm Optimization (PSO), FA Genetic Algorithm (GA), GWO, and WOA, respectively. These methods may fail to attain the best convergence for selecting the optimal placement of FACTS in a power system [40-43].

2. Related works

Many different methods are available to improve the security of the system and stability. Some of the works are reviewed in this section. Muhammad Nadeem et al. [13] have presented WOA for enhancing the stability problem by optimal FACTS location, for instance, UPFC, TCSC, and SVC. Optimal positioning of these FACTS devices is achieved by using WOA and implementing a system to reduce operating costs, including the cost of FACTS devices and active power loss. The presented method was validated with the consideration of IEEE 30 and the IEEE 14 bus system. The projected method was contrasted with PSO and GA. However, this method was not considered security constraints. Ayman alhejji et al. [14] have presented the Adaptive Grasshopper Optimization Algorithm (AGOA) to maintain system stability. The system power flow operation was enhanced by placing the Center Node Unified Power Flow Controller (C-UPFC). The device is located on the power grid, mainly on the transmission line, which improves independent voltage regulation, also the regulation of current flow. The presented method was implemented in spiral path formulation in search agents and levy flight distribution in the conventional grasshopper algorithm [44-46]. The projected method was validated by using IEEE 26, IEEE 57, and IEEE 30 bus systems. But, significant objectives of cost function were not taken in the system.

B. Vijayakumar et al. [15] have presented Runner Root Algorithm (RRA) with Chaotic Krill Herd (CKH) to improve the stable operation in the system. The projected method has been implemented with a combination of RRA and CKH so, it was named as CKHRA method. The presented method has been utilized to find the optimal location of UPFC in the transmission line when required by the FACTS device to reduce the power loss of the system. Two different objective functions were considered to maintain stable operation in the system. The low level of voltage deviation is also used to improve the stable operation. The presented method was employed in IEEE 30 and IEEE 14 bus systems. However, a hybrid technique was consuming a large time to provide the optimal location in the system.

Thang Trung Nguyen et al. [16] have presented a multi-objective genetic algorithm to recover the steady and dependable power system function. The support of a genetic algorithm achieved the multi-objective function. The offered technique was verified on the IEEE 30 system. It was then contrasted with a previously designed method such as Mixed Integer Non-Linear Program (MINLP), Differential Evolution (DE), and PSO. And, achieved outcomes provide fast convergence as well as accuracy in the proposed method. However, it was working with fast convergence but may be trapped in convergence. Partha P. Biswas et al. [17] have obtainable Success History-Based Adaptive Differential Evolution (SHADE) to solve power flow problems by optimizing FACTS devices. The presented approach was considered different objective functions such as reserve cost, penalty cost, direct cost, and thermal generation cost. In this method, the constraints were achieved with the Feasible Solutions (FS) method's superiority. However, this method does not consider the security constraints when checking the OPF power system issues [47-49].

The residual portion of the paper is prearranged as shadows. The proposed system model, along with its objectives and constraints, are presented in section 3. Additionally, it provides information related to optimization objective functions in a power system. The objective functions and security constraints details are explained in the sub-section of 3. The performance evaluation of the proposed methodology with simulation outcomes is obtainable in segment 5. The conclusion of the investigation related to security enhancement in the power system is presented in section 6.

3. Proposed System model for security enhancement

Recently, power system management, control, and system operations are considered the main difficult task by

enhancing the system's reliability, security, and stability. Failure and generator outage may happen during system operation conditions due to the system's failure. Other issues also happen, which completely collapse the security of the system. Hence, security enhancement is considered as the main motive of this research in the power system. The security of the system is enhanced through the location of FACTS devices inline transmission. Considered the four types of FACTS devices in the system to enable the system's security and reliability, such as UPFC, TCSC, SVC, and IPFC. When placing the suitable FACTS device in the transmission line, it surely degrades the stability issues and ensures security enhancements. The FACTS device placement mainly considers different types of objective functions such as power loss, voltage deviation, the investment cost of FACTS devices, fuel cost, severity index, and LOSI. Based on the objective functions, the best location of FACTS in the bus system is computed. The optimal selection is attained with the help of the ASO algorithm. This algorithm surely provides the greatest optimal placement of FACTS devices to improve the power flow with security constraints. The modeling of the FACTS is offered in the following segment.

3.1. Modelling of FACT devices

The research's main motive is to discover the optimal location of FACTS in the power system for reducing power loss and other objective functions. To attain the objective functions, the ASO algorithm is utilized. The optimal location of the FACTS device requires the knowledge of the modeling part. The mathematical modeling of selected FACTS devices is presented as follows.

3.1.1. UPFC

Gyugyi developed the UPFC in 1992, which used to enable the power flow of the system. The UPFC can change the power system's complete variables like angle, impedance, and voltage inside of buses, which changes the power system's power flow, especially in a transmission line. In the power system, it can be connected parallel and series in their transmission line. Hence, the UPFC device should use for both parallel and series compensators. Additionally, UPFC can control complete variables. But, the cost function of UPFC is considerable to use in the power system. In a system, the voltage compensation is required means, UPFC is best economical with their parallel compensators [20].
Additionally, if required the line impedances, the series compensator of UPFC is the best choice in the system. Finally, the UPFC has three-phase controllable bridges to switch power in the complete bus system. From figure 1, the modeling of UPFC is illustrated.

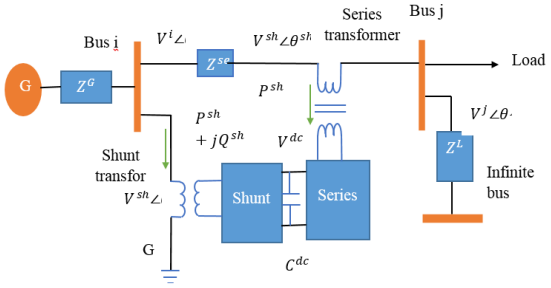

Figure 1. Mathematical design of UPFC device

The general design of UPFC structure developed among buses i and j respectively. The series and shunt controller are used to maintain a stable operation in a power system. In the UPFC, converter related by the transformer described with impedance such as load impedance, generator side impedance, shunt impedance, and series impedance [21]. The mentioned terms are need for enabling power flow operation in the system. The system power flow is enabled with the operation of series as well as shunt controller which formulated as follows,

$$P^{sh} + jQ^{sh} = V^{sh}\angle\theta^{sh}\left(\frac{V^{i}\angle\theta^{i} - V^{sh}\angle\theta^{sh}}{Z^{sh}}\right)^{*} \quad (1)$$

$$P^{ij} + jQ^{ij} = V^{i}\angle\theta^{i}\left(\frac{V^{i}\angle\theta^{i} - (V^{j}\angle\theta^{j} + (V^{se}\angle\theta^{se})}{Z^{se}}\right)^{*} \quad (2)$$

Where, $V^{j}\angle\theta^{j}$ and $V^{i}\angle\theta^{i}$ is labelled as voltage phase j and i, $V^{se}\angle\theta^{se}$ can be denoted as a voltage of series converter in UPFC, $V^{sh}\angle\theta^{sh}$ it denotes as a voltage of shunt converter in UPFC, Q^{ij} can be described as series converter reactive power flow in UPFC, P^{ij} can be described as shunt converter power flow in UPFC, Q^{sh} is described as shunt converter reactive power in UPFC and P^{sh} is described as series converter real power in UPFC. The UPFC series and shunt converter surely enhance the system's optimal power flow through active power exchanges. And, active power exchange has happened in the system through the dc link. The UPFC constraints are mathematically formulated as follows,

$$P^{se} - P^{sh} = 0 \quad (3)$$

Where, $P^{se} = re\,(V^{se}I^{ij})^{*}$ and $P^{sh} = re\,(V^{sh}I^{sh})^{*}$ can be described as exchange power of series and shunt converter in UPFC which attained with the consideration of dc-link capacitor.

TCSC

TCSC is designed with a capacitor bank connected in parallel to the thyristor. TCSC should be connected in a series manner in the transmission line. The TCSC reactance is mathematically formulated as follows,

$$X^{TCSC} = \frac{X^c \times X^l}{\frac{X^c}{\pi}[2(\pi - \alpha) + \sin(2\alpha)] - X^l} \quad (4)$$

The thyristor's firing angle X^l can be described as the reactor's reactance, X^c can be described as the capacitor's reactance [22]. The TCSC rating is installed, which consider as independent parameters and formulated as follows,

$$X^{TCSC} = R^{TCSC} \times X^{Line} \quad (5)$$

Where R^{TCSC} can be described as the degree of compensation and X^{Line} can be described as reactance of the transmission line. Additionally, the compensation degree limits are denoted among [-0.8, 0.2], which omits the critical condition of under and overcompensation. The TCSC reactance can be altered by adjusting the firing angle, which alters line reactance where it could be connected. The changes of reactance can be formulated as follows,

$$X_{new} = X_{old} + X^{TCSC} \quad (6)$$

Where X_{new} can be described as line reactance after location of TCSC and X_{old} can be described as line reactance before the location of TCSC.

3.1.2. SVC

SVC is utilized to given required reactive power in the transmission line when oscillations occur. SVC device contains a capacitor bank connected as a shunt and a pair of thyristors connected as anti-parallel. The shunt converter is connected when compensation is required in a transmission line. The SVC can provide capacitive or inductive compensation in the bus system [23]. The SVC reactive power compensation mathematically formulated as follows,

$$Q_{SVC} = -V_i^2 \times B_{SVC} \quad (7)$$

Where, B_{SVC} is defined as susceptance of the SVC, magnitude of voltage is denoted as V_i. The susceptance of the SVC can be formulated as follows,

$$B_{SVC} = \frac{X^l - \frac{X^c}{\pi}[(\pi - \alpha) + \sin(2\alpha)]}{X^c \times X^l} \quad (8)$$

Where α is defined as the firing angle of the thyristors, X^c can be described as reactance of capacitor and X^l can be is defined as reactance of the capacitor.

IPFC

Generally, IPFC contains two back-to-back converters connected with a DC link. Additionally, IPFC can manage the transmission line system real as well as reactive power flow. It is utilized to transfer real power from one line to a different line by the common dc link, injecting the required voltage in the transmission line [24]. When placing the IPFC in a transmission line, the complete power system stable operation and security also enhanced. The mathematical formulation of IPFC is presented as follows,

$$P^{ij} = (V^i)^2 X_{ii} - \sum_{j-1,j\neq i}^{N} V^i V^j (X_{ij} \cos\theta_{ij} - Y_{ij} \sin\theta_{ij} + \sum_{j-1,j\neq i}^{N} V^i Vse^{ij} (X_{ij} \cos(\theta_{ij} - \theta se_{ij}) - Y_{ij} \sin(\theta_{ij} - \theta se_{ij})) \quad (9)$$

$$Q^{ij} = (V^i)^2 Y_{ii} - \sum_{j-1,j\neq i}^{N} V^i V^j (X_{ij} \sin\theta_{ij} - Y_{ij} \cos\theta_{ij}) - \sum_{j-1,j\neq i}^{N} V^i Vse^j (X_{ij} \sin(\theta_{ij} - \theta se_{ij}) - Y_{ij} \cos(\theta_{ij} - \theta se_{ij})) \quad (10)$$

$$P^{ji} = (V^i)^2 X_{ii} - \sum_{j-1,j\neq i}^{N} V^i V^j (X_{ij} \cos(\theta_j - \theta_i) - Y_{ij} \sin(\theta_j - \theta_i)) - \sum_{j-1,j\neq i}^{N} V^i Vse^{ij} (X_{ij} \cos(\theta_{ij} - \theta se_{ij}) - Y_{ij} \sin(\theta_{ij} - \theta se_{ij})) \quad (11)$$

$$Q^{ji} = (V^i)^2 Y_{ii} - \sum_{j-1,j\neq i}^{N} V^i V^j (X_{ij} \sin(\theta_j - \theta_i) - Y_{ij} \cos(\theta_j - \theta_i)) - \sum_{j-1,j\neq i}^{N} V^i Vse^{ij} (X_{ij} \sin(\theta_j - \theta se_{ij})) - Y_{ij} \cos(\theta_{ij} - \theta se_{ij})) \, Re(Vse_{ij} . I^*_{ji} + Vse_{ik} . I^*_{ki}) \quad (12)$$

Where V^i and V^j represents the voltage magnitude constraint at bus i and j (p.u), Vse_{ijk} and I^*_{ijk} denotes the series voltage and reference current. The IPFC system completely enhances security.

3.2. Objective functions:

In this part, the multi-objective function's main necessity is to minimize or decrease actual real power loss, voltage deviation, severity index, LOSI, investment costs, fuel costs, and constraints with the employed technique. The used ASA algorithm obtains this. The objective function illustrates the proceeding equation (13),

$$[f] = \min f1 + f2 + f3 + f4 + f5 \quad (13)$$

Where f1, f2, f3, f4, f5 characterizes the objective function 1, 2, 3, 4, 5, and f symbolizes the objective function.

3.2.1. Real power loss

At this stage, the real power losses are minimized. In the network, a redistribution of reactive power is done due to the loss of transmit power. Thus, its minimization opens the way to modifying the actual power produced by the inactive bus. To reduce the actual power loss is the

preliminary objective function in the transmission line which is given in the below equation (14),

$$f_1 = p_{loss} = \sum_{\substack{k=1,\\ j\neq i}}^{n_{line}} X_{kj}\left[(V^k)^2 + (V^j)^2 - 2\,V^k.V^j\,\cos(\delta_k - \delta_j)\right] \quad (14)$$

Where δ_k and δ_j can be described as the angles of bus k also j, V^k and V^j represents voltages of the bus k and j, X_{kj} mentions the conductance among the bus k and j, n_{line} is the complete count of transmission lines also real power is indicated by p_{loss}.

3.2.2. Voltage deviation

In this section, the minimization of the variation of the load buses is carried out by the use of magnitude voltage which is illustrated in the given equation (15),

$$f_2 = V^{dev} = \sum_{i=1}^{n^l} \left| V^i - V_i^* \right| \quad (15)$$

Where, V_i^* is fixed as 1.0 p. u, and V_i^* corresponds the voltage magnitude current parameter at the ith load bus, the insignificant value of the magnitude voltage can be given by V^i, n^l represents the load buses.

3.2.3. Severity index

In this phase, minimizing the severity index of the system is done out. The function of the severity index is performed by the below-given equation (16),

$$f_3 = si = \sum_{L=l_0}^{N} \left(\frac{S_L}{S_L^{max}}\right)^{2M} \quad (16)$$

Where M represents the integer r exponent = 1, which is assumed, the overload lines set is mentioned as l_0, s_L^{max} stands for the line rating, s_L denotes the inline flow 1(MVA).

3.2.4. LOSI

In this phase, the Line overload sensitivity index (LOSI) can be introduced to detect the best place of UPFC, and thus this LOSI intended for every of the transmission lines is evaluated below certain contingencies. By consideration of several contingencies 'Nc', adding the flow of power in a line-i, and thus the LOSI parameter for a line i can be computed and formula for the calculation of LOSI intended for a presented load scenario is given by the following equation (17),

$$LOSI_i^{bl} = \sum_{n=1}^{n_C} \left(\frac{S_i^n}{S_i^{max}}\right) \quad (17)$$

Where the largest power flows in line-i and contingency flows of power can be represented by S_i^{max}, S_i^n.

3.2.5. Investment cost:

In the point of investment cost, one of the main objective functions of the FACTS appliances is the investment costs such as IPFC, UPFC, and the STATCOM in terms of ($/h) which is mean evaluated by the following equation (18),

$$f_5 = cost^{STATCOM} + cost^{UPFC} + cost^{IPFC} \quad (18)$$

Where,

$$cost^{STATCOM} = 0.0003\,S^2 - 0.3051S + 127.38$$

$$cost^{UPFC} = 0.0003\,S^2 - 0.026911S + 188.22$$

$$cost^{IPFC} = cost^{IPFCA} + cost^{IPFCB}$$

$$cost^{IPFCA} = 0.00015S_i^{\,2} - 0.01345S_i + 94.11$$

$$cost^{IPFCB} = 0.00015S_j^{\,2} - 0.01345S_j + 94.11$$

$$S = |R_2| - |R_1|$$
$$S_i = |R_{i2}| - |R_{i1}|$$
$$S_j = |R_{j2}| - |R_{j1}|$$

Where i implies both before and subsequent for setting up the IPFC in the MVAR, R_{i1} and R_{i2} represents the reactive flow of power in line, the converters linked to bus i and j cost function is determined by S_{ij}, R_1 symbolizes the reactive flow power in the line prior for setting up the FACTS in the MVAR, R_2 indicates the reactive power flow in the subsequent line towards setting up FACTS the MVAR.

3.2.6. Fuel cost

In this stage, fuel cost minimization is performed in the generator. The generator fuel cost principle represents the convex fuel cost functions involved by the quadratic cost. The quadratic fuel costs functions in the generating units are demonstrated in equation (19) which is as given below,

$$f_6 = \text{mincost}^F(X) = \sum_{i=1}^{n_G} [A^i (p^{gi})^2 + B^i p^{gi} + C^i] \quad (19)$$

Where p^{gi} corresponds the ith generator limit of the active power generator, ith generator fuel costs coefficients are given by A^i, B^i, C^i, i denotes the bus number index, and the number of generators is described by n_G.

3.3. Constraints

The projected optimization equality and inequality constraints issue is tackled successfully utilizing the following constraints: FACTS device limits, Reactive power generation limits, Real power generation limits, security constraints, voltage constraints, and load flow constraints.

3.3.1. FACTS device limits:

The FACTS device limits are revealed in the equation (20) given below,

$$\left.\begin{array}{l} x_f^{min} \le x_f \le x_f^{max} \\ v_{Vr}^{min} \le v_{Vr} \le v_{Vr}^{max} \\ v_{Cr}^{min} \le v_{Cr} \le v_{Cr}^{max} \\ \delta_{Vr}^{min} \le \delta_{Vr} \le \delta_{Vr}^{max} \\ \delta_{Cr}^{min} \le \delta_{Cr} \le \delta_{Cr}^{max} \end{array}\right\} \quad (20)$$

Where x_f determines the reactance of q_{gi}^{max} and FACTS devices.

3.3.2. Reactive power generation limits

The reactive power generation boundaries are effectively demonstrated in the following equation (21)

$$q_{gi}^{min} \le q_{gi,T} \le q_{gi}^{max}, gi \in n_{gi} \quad (21)$$

Where, n_{gi} denotes the number of generator buses, the maximum and the maximum bounds for the generation of reactive power for unit i are determined $q_{gi}^{min}, q_{gi}^{max}$.

3.3.3. Real power generation limits

The real power generation limits are illustrated by the equation (22), which is given as follows

$$p_{gi}^{min} \le p_{gi,T} \le p_{gi}^{max}, gi \in n_{gi} \quad (22)$$

Where n_{gi} implies the number of generator buses.

3.3.4. Security constraints:

The security constraints are determined in equations (23) and (24)

$$(V^i)^{min} \le V^{i,t} \le (V^i)^{max}, i \in n_{bus-1} \quad (23)$$

$$|bf^{(i,T)}| \le (bf^i)^{max}, i \in n_{bus} \quad (24)$$

Where $(bf^i)^{max}$ illustrates the maximum limits for the power flow branch i (MVA), $bf^{(i,T)}$ symbolizes the branch flow of power at i time t (MVA), the number of buses excluding the slack bus is characterized by n_{bus}, n_{bus-1}.

3.3.5. Voltage constraints:

The given equation (25) defines the magnitude voltage limits at all the buses,

$$\left.\begin{array}{l} (V^i)^{min} \le V^i \le (V^i)^{max}, i = 1,2,\ldots.., n_{bus} \\ (V^j)^{min} \le V^j \le (V^j)^{max}, j = 1,2,\ldots.., n_{bus} \end{array}\right\} \quad (25)$$

3.3.6. Load flow constraints:

The load flow constraints are duly performed in the below-given equation (26)

$$\left.\begin{array}{l} q_i - V^i \sum_{j=1}^{n_{bus}} V^j (X_{ij} \sin\theta_{ij} - Y_{ij} \cos\theta_{ij}) = 0, \ i = 1,2,.,n_{pq} \\ p_i - V^i \sum_{j=1}^{n_{bus}} V^j (X_{ij} \cos\theta_{ij} + Y_{ij} \sin\theta_{ij}) = 0, \ i = 1,2\ldots,n_{bus-1} \end{array}\right\} \quad (26)$$

Where the number of buses is given by n_{pq}.

3.4. Atom Search Optimization to select the optimal location of FACT devices

Every substance is composed of an infinite number of atoms which moves in all directions at all time. This part introduces a new optimization algorithm called ASO, enthused with the consideration of molecular subtleties. Each atom has a definite distance between them, and according to that, the atoms attract or repel each other. This motivates the brighter atoms to forward towards the weightier ones [18]. A mathematical algorithm is acquired by the atoms' movement known as Atom Search Algorithm (ASA). These such atoms move with an acceleration such as given,

$$A = \frac{(fi + gi)}{Mi} \quad (27)$$

A represents the acceleration of atoms' movement, Mi represents the atom's mass, gi represents the constraint force of the atom, and fi represents the interaction of force.

Depending on the total force of the atom, a group of atoms can be designated to be the best group in the dth dimension to improve the exploration of atoms, and it is given by,

$$X^a i(o) = \sum_{j \in K_{best}} X^a ij(o) \quad (28)$$

where K_{best} is the best atom that was selected.

In the best atom and the population, between every atom, there is a covalent bond in which a constraint force is subjected in each atom that consequences after the finest atom at each iteration in the algorithm and thus this restraint force is given as,

$$\theta_i(y) = \left[|a_i(y) - a_{best}(y)|^2 - b_{i,best}{}^2 \right] \quad (29)$$

The constant length of the bond between the best one and the ith atom $a_{best}(y)$ represents the optimal atom's location at the iteration (y). Thus, the constraint force on an ith atom is determined by

$$H^d{}_i(x) = \lambda(x) \left(a^d{}_{best}(x) - a^d{}_i(x) \right) \quad (30)$$

Where $\lambda(x)$ acts as a Lagrangian multiplier.

$$\lambda(x) = \beta e^{-\frac{20T}{t}} \quad (31)$$

where β represents the weight of the multiplier. Then, the fitness value can be given by,

$$fit_{best}(x) = \min fit_i(x) \quad (32)$$

Where i denotes the order of the atom in the population.

To enhance and enhance the atom's exploration in the projected algorithm, the atoms in the initial iterations stab to interrelate with numerous additional particles with its nationals consume healthier suitability value [19]. At the last iterations, to increase the exploitation, the atoms interrelate with fewer nationals' atoms with healthier suitability values.

4. Performance evaluation

Our proposed method's performance evaluation is evaluated in this part, and the case scenarios with their graphs are verified. The proposed methodology has been utilized to enhance the security system and identify the FACTS devices' optimal placement in the power system. The categories of FACTS devices that can be assumed are UPFC, TCSC, SVC, and IPFC. The transmission line that has the maximum and reactive power executes these FACT appliances. By selecting the line that carries the large reactive power, the FACT appliances' exact location is picked out. The exact location is selected for the FACT devices such as UPFC, TCSC, SVC, and IPFC with IEEE 30, IEEE 118, IEEE 300. The implemented Atom Search Algorithm is effectively executed on the IEEE 30 and IEE 118.

Additionally, IEE 300 depends on the optimization technique employed elegantly, which is utilized to access the optimum magnitude of FACTS appliances at pre-set locations. The system performances are performed both with and without FACT appliances. The proposed novel technique is compared with existing techniques such as GWO, WOA, DA, FPA, Jaya, JA-FPA. Table 1 implies the proposed technique performance factors with that of the existing techniques mentioned

Table 1. Implementation parameters of proposed and existing techniques.

Method	Description	Parameters
ASA	Iteration	100
	Population	50
	Multiple weight	0.5
	Depth weight	10
GWO	Number of search agents	30
	Maximum iteration	100
	Dimension	5
FPA	Maximum iteration	200
	Switching probability (P)	0.6
	No. of runs	30

4.1. Case 1:

Performance Analysis of the IEEE 30 bus system

In this segment, the efficiency of the proposed technique is executed by including various tests is analyzed. In this work, towards improving the system's security and identifying an optimal location or position for the FACTS devices with the utilization of our proposed system. The FACTS devices are such as UPFC, TCSC, SVC, IPFC. The proposed technique is performed with IEEE 30 bus system to analyze the performance of the objective functions such as severity index, LOSI, voltage, voltage deviation, power loss, fitness, and fuel cost are evaluated and contrasted with that of the proposed system. Figure 2 depicts the basic structure of the IEEE 30 bus system, as in table 2.

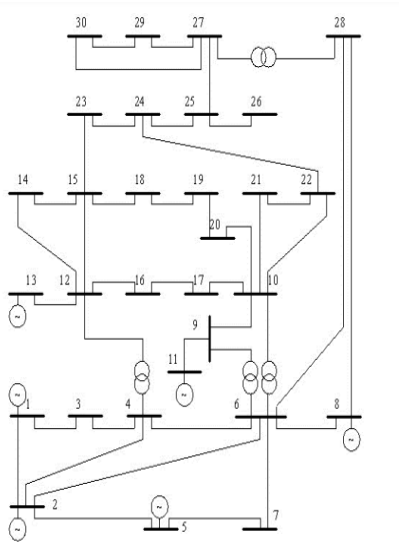

Figure 2. Basic structure of the IEEE 30 bus system

Table 2. IEEE 30 bus system generator and cost coefficients

Generator bus no		1	2	5	8	11	13
P_G^{min} MW		50	20	15	10	10	12
P_G^{max} MW		200	80	50	35	30	40
Fuel cost coefficients	a_i	0.00	0.00	0.00	0.00	0.00	0.00
	b_i	2.00	1.75	1.00	3.25	3.00	3.00
	c_i	0.00 38	0.01 75	0.06 25	0.00 83	0.02 50	0.02 50

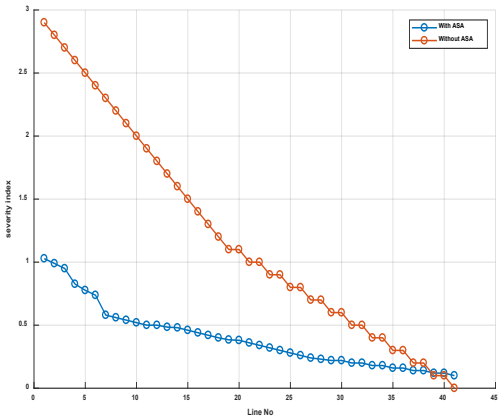

Figure 3. Analysis of Severity index

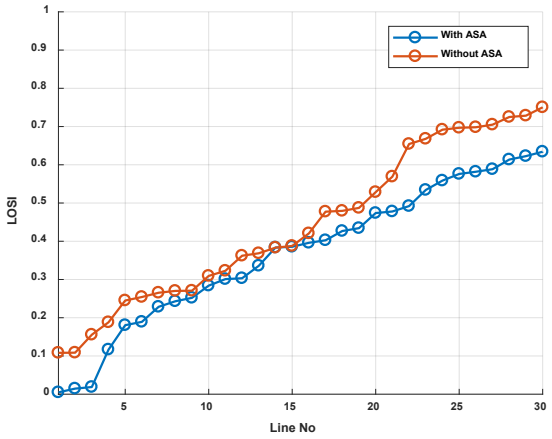

Figure 4. Analysis of LOSI

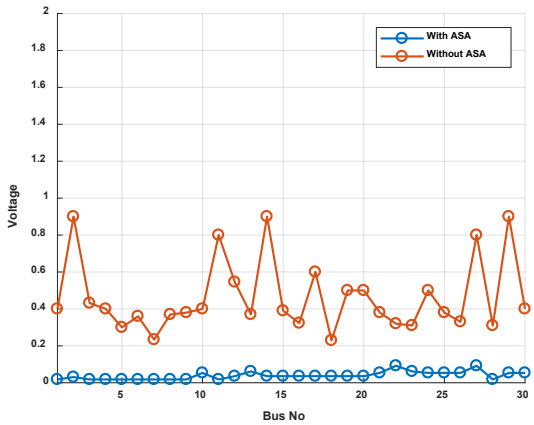

Figure 5. Analysis of voltage

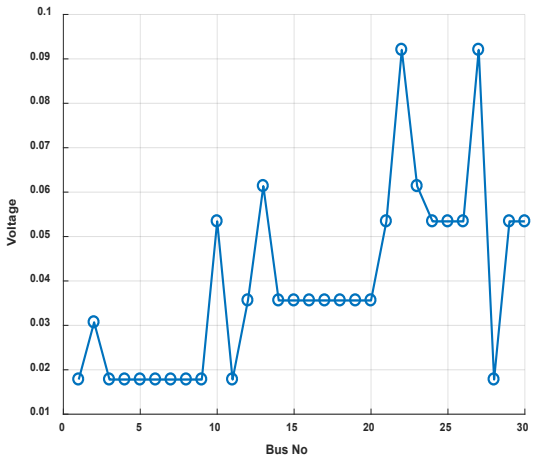

Figure 6. Analysis of voltage deviation

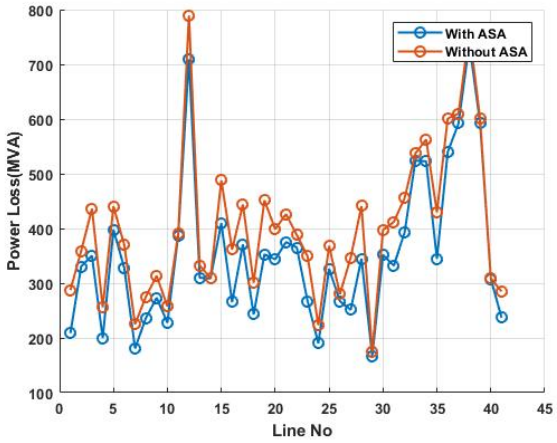

Figure 7. Analysis of Power-loss

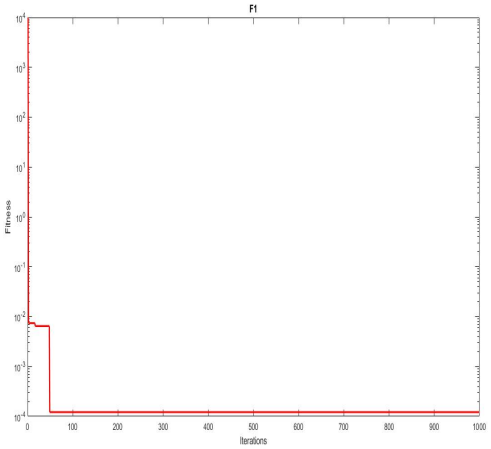

Figure 8. Analysis of fitness function

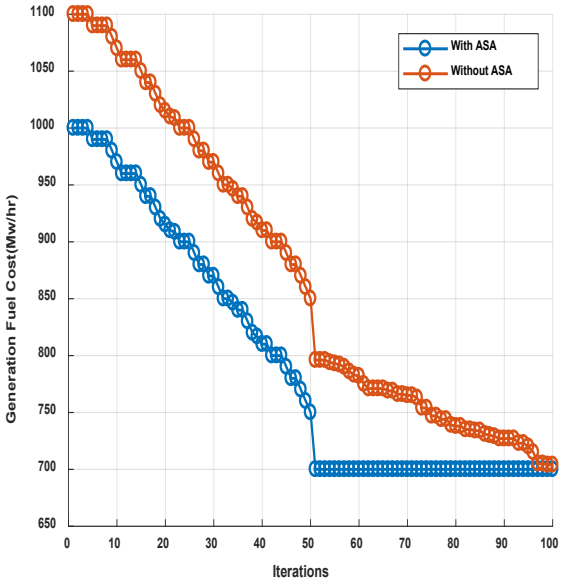

Figure 9. Analysis of Fuel cost

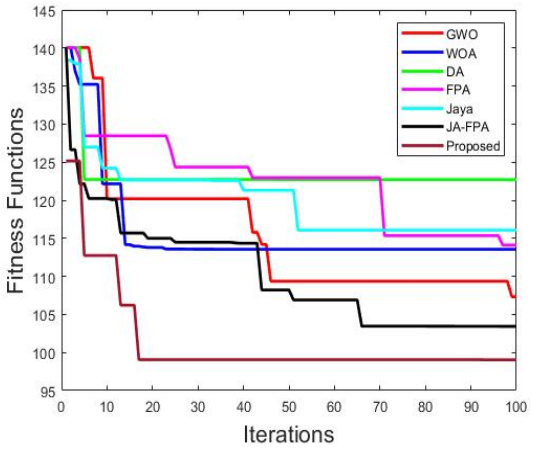

Figure 10. Comparative analysis of fitness functions of the proposed system with other existing systems

From the graphs plotted analysis, it is clear that from figure 3, the proposed system severity index attains 0.03as the higher value at bus no.10 and the least value as 0.01 in bus no.0-10 in IEEE 30 bus system. With figure 4, LOSI analysis is obtained, and thus, the highest value attained is 0.5 in between the bus no.15-20, and the lowest value obtained is 0 from bus no. 0-9 at IEEE 30 bus system. From figure 5, the voltage analysis is achieved as the high value of 0.092 in bus no.27, and the low value is attained at 0.02 from bus no.3-9 at IEEE 30 bus system. The voltage deviation analysis attains the high value as 360 in bus no.0 while the low value as 340 in bus no.30 at IEEE 30 bus system is presented in Figure 6. Figure 7 illustrates the analysis of power loss in which 0.15 in bus no.27 is the highest value when the lowest value is 0.01 in bus no.5 at IEEE 30 bus system. The fitness function evaluation is demonstrated in figure 8, in which the higher value is 104 at iteration 0, while the lower value is 10-4 at iteration 1000 at IEEE 30 bus system. Figure 9 helps analyze fuel cost in which the high value attained is 5500 at bus no.27 while the low value attained is 750 in bus no.5 at IEEE 30bus system. With the graphs plotted and the comparative analysis obtained, the proposed system attains 100 at iterations 20. In contrast, the existing system JA-FPA attained the cost is 140 at the iterations 65, the Jaya system attained cost was 137 at the iterations 50 when the FPA system attained the cost is 140 at iterations 98, the DA system attained the cost of 140 at the iterations 5, the WOA system attained the cost value 140 at the iterations 15. Finally, the GWA system attained the cost value of 140 at iterations 99. Thus with the above analysis, it is concluded that the proposed system has the least cost parameters when contrasted with that of the other conventional systems such as JA-FPA, Jaya, FPA, DA, WOA, and the GWA systems, as in figure 10.

4.2. Case.2: Analysis of IEEE 118 bus system.

This section is presented the performance analysis of the IEEE 118 bus system is evaluated and verified. The

efficiency of the proposed method is executed by including various tests is analyzed. In this work, to improve system security, we also identify an optimal location or position for the FACTS devices to utilize our proposed system. The FACTS devices are UPFC, TCSC, IPFC, SVC. The proposed technique is performed with an IEEE 118 bus system intended to analyze objective functions such as severity index, LOSI, voltage, voltage deviation, power loss, fitness function, and fuel cost are evaluated and contrasted with that of the proposed system.

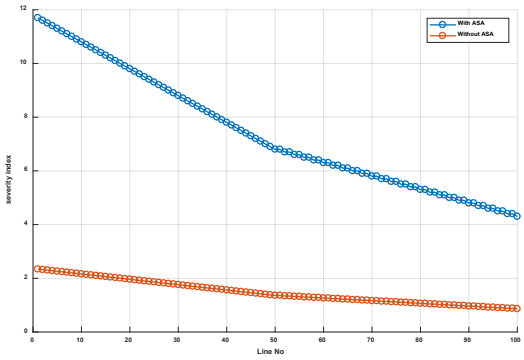

Figure 11. Analysis of Severity index

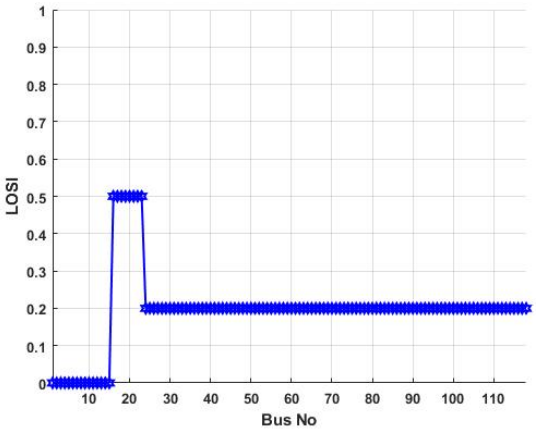

Figure 12. Analysis of LOSI

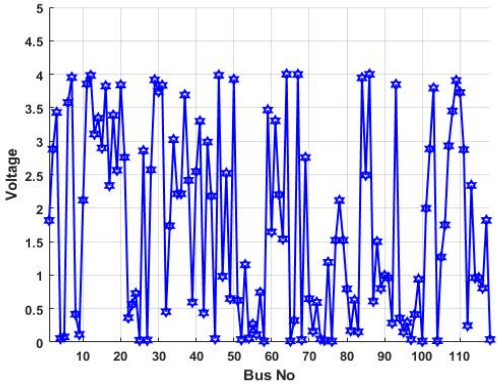

Figure 13. Analysis of Voltage

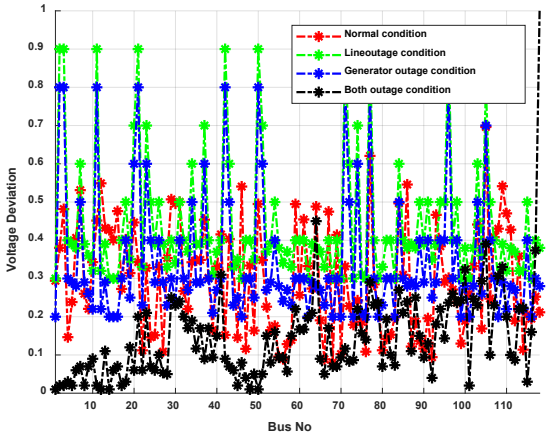

Figure 14. Analysis of Voltage deviation

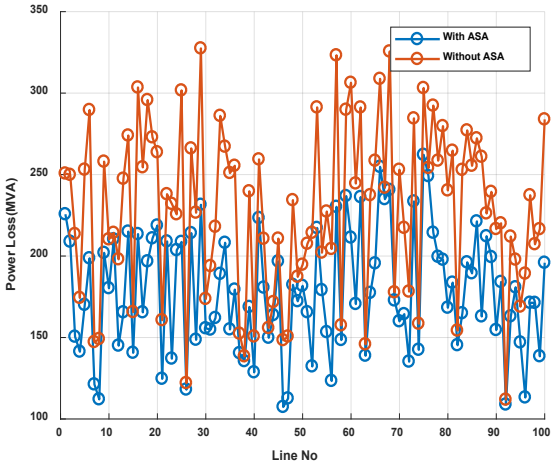

Figure 15. Analysis of Power loss

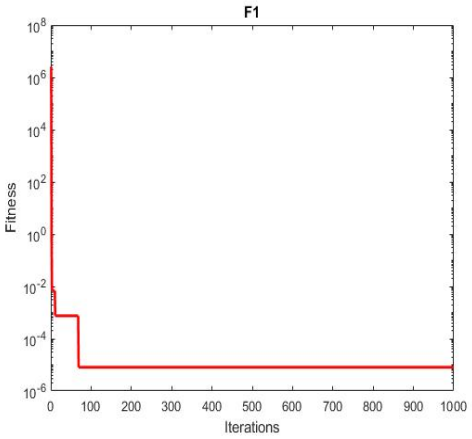

Figure 16. Analysis of Fitness function

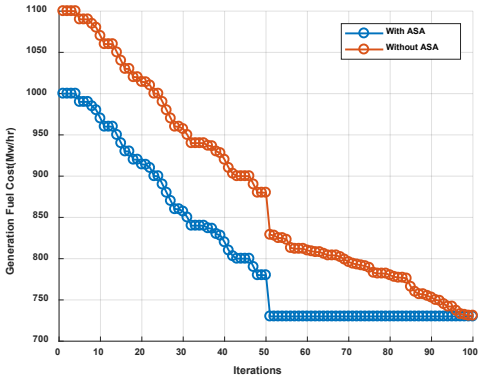

Figure 17. Analysis of Fuel cost

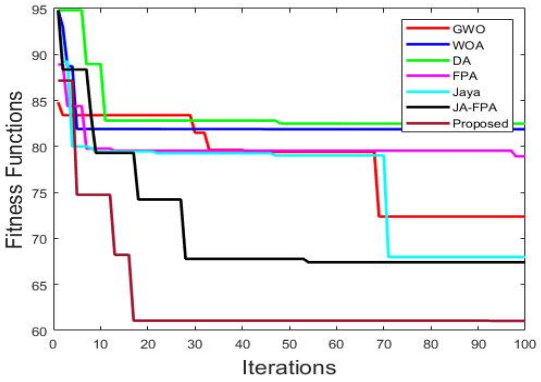

Figure 18. Comparative analysis of the fitness functions of our proposed system with an existing system

From the graphs plotted analysis, it is clear that from figure 11, the proposed system severity index attains 0.01 as the higher value at bus no.52 and the least value as 0 in bus no.22 in IEEE 118 bus system. In figure 12, the LOSI analysis is also obtained; thus, the highest value attained is 0.5 in between the bus no.20, and the lowest value obtained is 0 from bus no.10 at IEEE 118 bus system. From figure 13, the voltage analysis is achieved as the high value of 4 in bus no.50, and the low value is attained at 0 from bus no.5 at IEEE 118 bus system. The voltage deviation analysis attains the high value as 360 in bus no.0 while the low value as 280 in bus no.110 at the IEEE 118 bus system, presented in Figure 14. Figure 15 illustrates an analysis of power loss in which 0.8 in bus no, 32 is the highest value when the lowest value is 0.05 in bus no.82 at the IEEE 118 bus system. The fitness function analysis is demonstrated in figure 16, in which the higher value is 107 at iteration 0, while the lower value is 10-5 at iteration 80 at IEEE 118 bus system. Figure 17 helps analyze the fuel cost in which the high value attained is 6.1✕104 at bus no.112 while the low value attained is 0 in bus no.40 at IEEE 118 bus system. With the analysis of the graphs plotted and comparative analysis obtained, the proposed system attains 61 at iterations figure 18.

In contrast, the existing system JA-FPA attained the cost is 67 at the iterations 55, the Jaya system attained cost was 69 at the iterations 70 when the FPA system attained the cost is 79 at iterations 98, the DA system attained the cost of 83 at the iterations 50, the WOA system attained the cost value 82 at the iterations 5. Finally, the GWA system attained the cost value of 73 at iterations 70. Thus, with the above analysis, it is concluded that the proposed system has the least cost parameter when contrasted with that of the other conventional systems such as JA-FPA, Jaya, FPA, DA, WOA, and the GWA systems.

4.3. Case.3: Analysis of IEEE 300 bus system.

This section is presented the performance analysis of the IEEE 300 bus system is evaluated and verified. The efficiency of the suggested method is executed by including various tests is analyzed. In this work, to enhance the system security and identify an optimal location or position for the FACTS devices with our proposed system's utilization. The FACTS devices are such as UPFC, TCSC, SVC, IPFC. The proposed technique is performed with IEEE 300 bus system to analyze the performance of objective functions such as severity index, LOSI, voltage, voltage deviation, power loss, fitness function, and fuel cost are evaluated and contrasted with that of the proposed system.

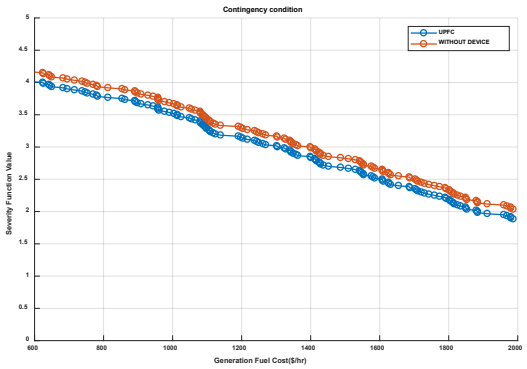

Figure 19. Analysis of severity index

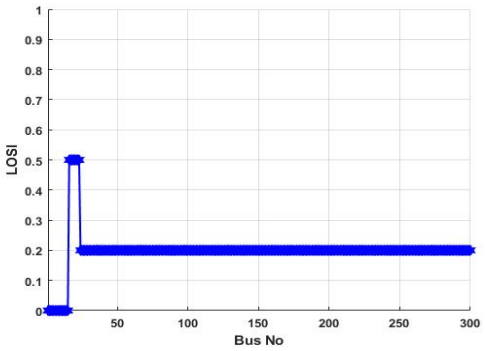

Figure 20. Analysis of LOSI

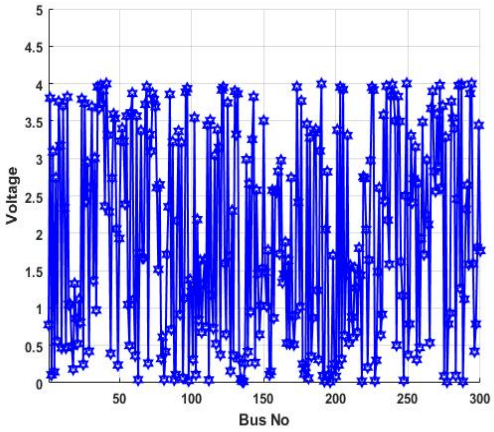

Figure 21. Analysis of Voltage

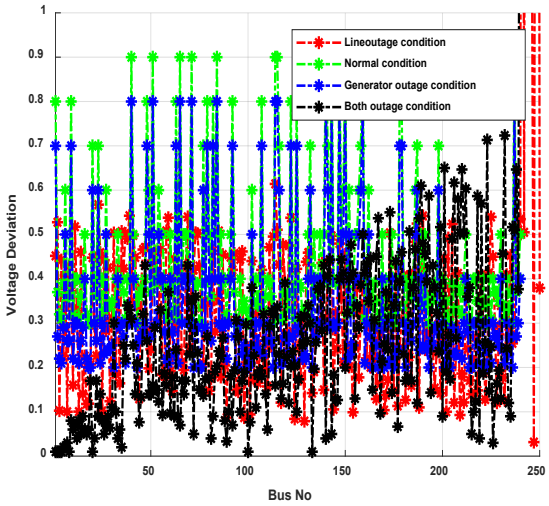

Figure 22. Analysis of Voltage deviation

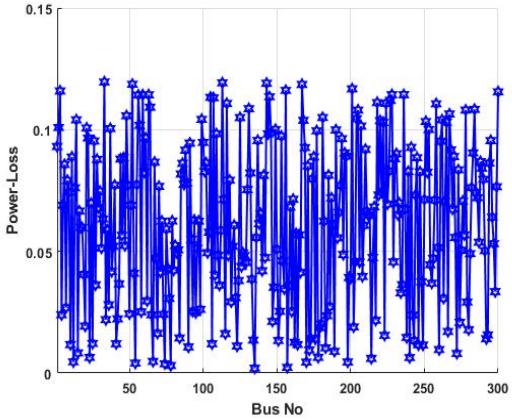

Figure 23. Analysis of Power-loss

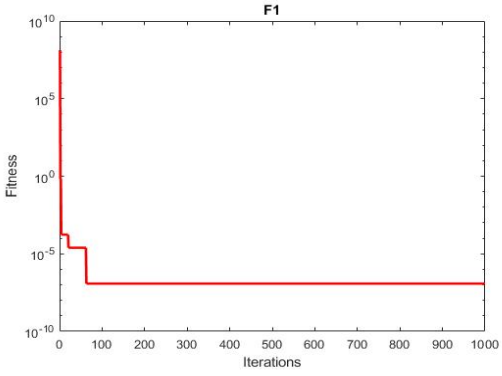

Figure 24. Analysis of fitness function

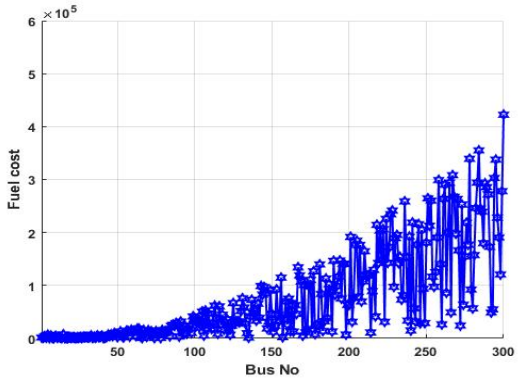

Figure 25. Analysis of Fuel cost

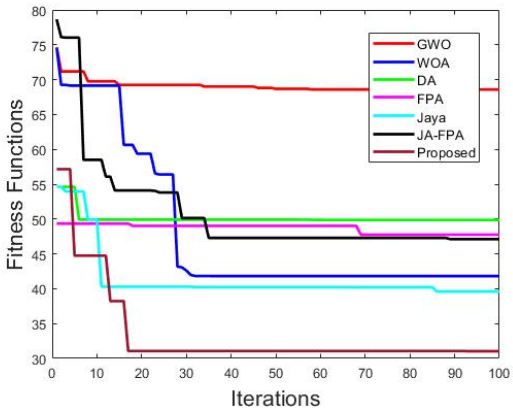

Figure 26. Comparative analysis of the fitness functions of the proposed system with existing systems.

From the graphs plotted analysis, it is clear that from figure 19, the proposed system severity index attains 0.01 as the higher value at bus no.50 and the least value as 0 at bus no. 160 in IEEE 300 bus system. In figure 20, the analysis of LOSI is obtained, and thus, the highest value attained is 0.5 at the bus no. 20 and the lowest value obtained is 0 from bus no.10 at IEEE 300 bus system. From figure 21, the voltage analysis is achieved as the high value of 4 in bus no.250, and the low value is attained at 0 from bus no. 70 at IEEE 300 bus system. The voltage deviation analysis attains the high value as 360 in bus no.0 while the low value as 210 in bus no.300 at the IEEE 300 bus system, shown in Figure 22. Figure 23

illustrates the analysis of power loss in which 0.8 in bus no.30 is the highest value when the lowest value is 0 in bus no.140 at the IEEE 300 bus system. The fitness function analysis is demonstrated in figure 24, in which the higher value is 108 at iteration 0, while the lower value is 10-7 at iteration 60 at IEEE 300 bus system. Figure 25 helps analyze the fuel cost in which the high value attained is 4.2105 at bus no.300 while the low value attained is 0 in bus no.50 at the IEEE 300 bus system. By analyzing the graphs plotted and the comparative analysis obtained, the proposed system attains 31 at iterations 18.
In contrast, the existing system JA-FPA attained the cost is 47 at the iterations 38, the Jaya system attained cost was 39 at the iterations 85 when the FPA system attained the cost is 70 at iterations 49, the DA system attained the cost of 50 at the iterations 9, the WOA system attained the cost value 42 at the iterations 32. Finally, the GWA system attained a cost value of 70 at iterations 35. Thus, with the above analysis, it is concluded that the proposed system has the least cost value when compared with that of the other existing systems such as JA-FPA, Jaya, FPA, DA, WOA, and the GWA systems, as in figure 26.

5. Conclusion

In this paper, ASA's developed method has been implemented to enhance the system's security by selecting the optimal location of FACTS devices. Here, the FACTS device's exact optimal location has been efficiently predicted with the ASA algorithm's help. To enhance the power system's security system, the FACTS devices must be positioned in the system's exact position. The FACTS devices assumed in the power system to enable the system's security are UPFC, TCSC, SVC, and IPFC. The exact placement of the FACTS devices related to the various types of objective functions are investment costs, fuel costs, real power loss, voltage deviation, severity index, LOSI, and constraints with the employed technique are been evaluated with IEEE 30, IEEE 118, and IEEE 300 bus systems using its cost fitness functions. Objective functions compute the optimal location of the FACTS devices in the bus system. The support of the ASO algorithm obtains this optimal placement selection. The proposed methodology has been compared with other existing techniques such as JA-FPA, Jaya, FPA, DA, WOA, and GWA systems. The results and the comparative analysis obtained, the proposed method attains the least cost fitness functions compared to the other existing techniques. The proposed method evaluated validations are given in the comparison analysis part of the paper. Based on the comparative analysis obtained, it is strong that the proposed technique achieved the best outcomes and results. In the future, power transmission network system as a recommendation to reduce the power system and maintain system stability.

References

[1]. Srilakshmi, Koganti, P. Ravi Babu, and P. Aravindhababu. "An enhanced most valuable player algorithm based optimal power flow using Broyden's method." Sustainable Energy Technologies and Assessments 42 (2020): 100801.

[2]. Kyesswa, Michael, Alexander Murray, Philipp Schmurr, Hüseyin Çakmak, Uwe Kühnapfel, and Veit Hagenmeyer. "Impact of grid partitioning algorithms on combined distributed AC optimal power flow and parallel dynamic power grid simulation." IET Generation, Transmission & Distribution (2020).

[3]. Guerrero, Jaysson, Daniel Gebbran, Sleiman Mhanna, Archie C. Chapman, and Gregor Verbič. "Towards a transactive energy system for integration of distributed energy resources: Home energy management, distributed optimal power flow, and peer-to-peer energy trading." Renewable and Sustainable Energy Reviews 132 (2020): 110000.

[4]. Pan, Xiang, Minghua Chen, Tianyu Zhao, and Steven H. Low. "DeepOPF: A Feasibility-Optimized Deep Neural Network Approach for AC Optimal Power Flow Problems." arXiv preprint arXiv:2007.01002 (2020).

[5]. Pan, Xiang, Tianyu Zhao, Minghua Chen, and Shengyu Zhang. "Deepopf: A deep neural network approach for security-constrained dc optimal power flow." IEEE Transactions on Power Systems (2020).

[6]. Venzke, Andreas, Guannan Qu, Steven Low, and Spyros Chatzivasileiadis. "Learning optimal power flow: Worst-case guarantees for neural networks." arXiv preprint arXiv:2006.11029 (2020).

[7]. Lee, Dongchan, Konstantin Turitsyn, Daniel Kenneth Molzahn, and Line Roald. "Feasible path identification in optimal power flow with sequential convex restriction." IEEE Transactions on Power Systems (2020).

[8]. Muhammad, Yasir, Rahimdad Khan, Muhammad Asif Zahoor Raja, Farman Ullah, Naveed Ishtiaq Chaudhary, and Yigang He. "Design of fractional swarm intelligent computing with entropy evolution for optimal power flow problems." IEEE Access 8 (2020): 111401-111419.

[9]. Xia, Shiwei, Mohammad Shahidehpour, Ka Wing Chan, Siqi Bu, and Gengyin Li. "Transient Stability-Constrained Optimal Power Flow Calculation with Extremely Unstable Conditions using Energy Sensitivity Method." IEEE Transactions on Power Systems (2020).

[10]. Alhejji, Ayman, Mohamed Ebeed Hussein, Salah Kamel, and Saeed Alyami. "Optimal power flow solution with an embedded center-node unified power flow controller using an adaptive grasshopper optimization algorithm." IEEE Access 8 (2020): 119020-119037.

[11]. Avramidis, Iason-Iraklis, Florin Capitanescu, and Geert Deconinck. "Practical approximations and heuristic approaches for managing shiftable loads in the multi-period optimal power flow framework." Electric Power Systems Research 190 (2020): 106864.

[12]. Zhao, Tianyu, Xiang Pan, Minghua Chen, Andreas Venzke, and Steven H. Low. "DeepOPF+: A Deep Neural Network Approach for DC Optimal Power Flow for Ensuring Feasibility." arXiv preprint arXiv:2009.03147 (2020).

[13]. Nadeem, Muhammad, Kashif Imran, Abraiz Khattak, Abasin Ulasyar, Anamitra Pal, Muhammad Zulqarnain Zeb, Atif Naveed Khan, and Malhar Padhee. "Optimal Placement, Sizing and Coordination of FACTS Devices in

Transmission Network Using Whale Optimization Algorithm." Energies 13, no. 3 (2020): 753.
[14]. Alhejji, Ayman, Mohamed Ebeed Hussein, Salah Kamel, and Saeed Alyami. "Optimal power flow solution with an embedded center-node unified power flow controller using an adaptive grasshopper optimization algorithm." IEEE Access 8 (2020): 119020-119037.
[15]. Vijayakumar, B., G. Rajendar, and Veerlapati Ramaiah. "Optimal location and capacity of Unified Power Flow Controller based on chaotic krill herd blended runner root algorithm for dynamic stability improvement in power system." International Journal of Numerical Modelling: Electronic Networks, Devices and Fields (2020): e2828.
[16]. Nguyen, Thang Trung, and Fazel Mohammadi. "Optimal placement of TCSC for congestion management and power loss reduction using multi-objective genetic algorithm." Sustainability 12, no. 7 (2020): 2813.
[17]. Biswas, Partha P., Parul Arora, R. Mallipeddi, P. N. Suganthan, and B. K. Panigrahi. "Optimal placement and sizing of FACTS devices for optimal power flow in a wind power integrated electrical network." Neural Computing and Applications (2020): 1-22.
[18]. Kamel, Salah, Hanan Hamour, Mohammed Hassan Ahmed, and Loai Nasrat. "Atom Search optimization Algorithm for Optimal Radial Distribution System Reconfiguration." In 2019 International Conference on Computer, Control, Electrical, and Electronics Engineering (ICCCEEE), pp. 1-5. IEEE, 2019.
[19]. Zhao, Weiguo, Liying Wang, and Zhenxing Zhang. "A novel atom search optimization for dispersion coefficient estimation in groundwater." Future Generation Computer Systems 91 (2019): 601-610.
[20]. Rao, V. Srinivasa, and R. Srinivasa Rao. "Optimal placement of STATCOM using two stage algorithm for enhancing power system static security." Energy Procedia 117 (2017): 575-582.
[21]. Acharjee, P. "Optimal power flow with UPFC using security constrained self-adaptive differential evolutionary algorithm for restructured power system." International Journal of Electrical Power & Energy Systems 76 (2016): 69-81.
[22]. Duong, ThanhLong, Yao JianGang, and VietAnh Truong. "A new method for secured optimal power flow under normal and network contingencies via optimal location of TCSC." International Journal of Electrical Power & Energy Systems 52 (2013): 68-80.
[23]. Rao, B. Venkateswara, GV Nagesh Kumar, M. Ramya Priya, and P. V. S. Sobhan. "Optimal power flow by Newton method for reduction of operating cost with SVC models." In 2009 International Conference on Advances in Computing, Control, and Telecommunication Technologies, pp. 468-470. IEEE, 2009.
[24]. Ebeed, Mohamed, Salah Kamel, and Francisco Jurado. "Determination of IPFC operating constraints in power flow analysis." International Journal of Electrical Power & Energy Systems 81 (2016): 299-307.
[25]. Yeshitela Shiferaw, and K. Padma. "Enhancement of Power Flow with Reduction of Power Loss Through Proper Placement of FACTS Devices Based on Voltage Stability Index." In International Conference on Advances of Science and Technology, pp. 355-365. Springer, Cham, 2019.
[26]. Elias Mandefro, and Belachew Bantiyrga. "Optimal Allocation of Distributed Generation for Performance Enhancement of Distribution System Using Particle Swarm Optimization." In International Conference on Advances of Science and Technology, pp. 436-453. Springer, Cham, 2019.
[27]. Nebiyu Yisaye, Elias Mandefro, and Belachew Bantyirga. "Performance Enhancement of Distribution Power System by Optimal Sizing and Sitting of Distribution Statcom." In International Conference on Advances of Science and Technology, pp. 395-414. Springer, Cham, 2019.
[28]. Mingu Kang, and Ramon Zamora. "Optimal placement and sizing of DG and shunt capacitor for power loss minimization in an islanded distribution system." In International Conference on Smart Grid Inspired Future Technologies, pp. 43-52. Springer, Cham, 2018.
[29]. D Datta, S Mishra, SS Rajest, (2020) "Quantification of tolerance limits of engineering system using uncertainty modeling for sustainable energy" International Journal of Intelligent Networks, Vol.1, 2020, pp.1-8, https://doi.org/10.1016/j.ijin.2020.05.006
[30]. S. K. Khan, U. Naseem, H. Siraj, I. Razzak, and M. J. I. W. C. Imran, "The role of unmanned aerial vehicles and mmWave in 5G: Recent advances and challenges," Transactions on Emerging Telecommunications Technologies, p. e4241.
[31]. Vijai C.& Wisetsri, W. Rise of Artificial Intelligence in Healthcare Startups in India. Advances In Management. 14 (1) March (2021):48-52, 2021.
[32]. Patel, C.I.; Labana, D.; Pandya, S.; Modi, K.; Ghayvat, H.; Awais, M. Histogram of Oriented Gradient-Based Fusion of Features for Human Action Recognition in Action Video Sequences. Sensors 2020, 20, 7299. https://doi.org/10.3390/s20247299
[33]. Ghayvat, H.; Awais, M.; Pandya, S.; Ren, H.; Akbarzadeh, S.; Chandra Mukhopadhyay, S.; Chen, C.; Gope, P.; Chouhan, A.; Chen, W. Smart Aging System: Uncovering the Hidden Wellness Parameter for Well-Being Monitoring and Anomaly Detection. Sensors 2019, 19, 766, impact factor: 3.275, H-Index: 153, Scopus Q1. https://doi.org/10.3390/s19040766.
[34]. Sur S., Pandya, S., Ramesh P. Sah, Ketan Kotecha & Swapnil Narkhede, Influence of bed temperature on performance of silica gel/methanol adsorption refrigeration system at adsorption equilibrium, Particulate Science and Technology, Taylor and Francis, impact factor: 1.7, 2020. DOI: 10.1080/02726351.2020.1778145
[35]. Barot, V., Kapadia, V., & Pandya, S., QoS Enabled IoT Based Low Cost Air Quality Monitoring System with Power Consumption Optimization, Cybernetics and Information Technologies, 2020, 20(2), 122-140.
[36]. D.K. Sharma and D.S. Hooda, "Generalized Measures of 'Useful' Relative Information and Inequalities" Journal of Engineering, Management & Pharmaceutical Sciences, Vol.1(1), pp.15-21, 2010.
[37]. U. Naseem, M. Khushi, S. K. Khan, K. Shaukat, and M. A. Moni, "A Comparative Analysis of Active Learning for Biomedical Text Mining," Applied System Innovation, vol. 4, no. 1, p. 23, 2021
[38]. Naseem, U., Khan, S. K., Razzak, I., & Hameed, I. A. (2019, December). Hybrid words representation for airlines sentiment analysis. In Australasian Joint Conference on Artificial Intelligence (pp. 381-392). Springer, Cham.
[39]. Dilip Kumar Sharma, "Some Generalized Information Measures: Their characterization and Applications", Lambert Academic Publishing, Germany, 2010. ISBN: 978-3838386041.

[40]. S. K. Khan, M. Farasat, U. Naseem, and F. Ali, "Performance evaluation of next-generation wireless (5G) UAV relay," Wireless Personal Communications, vol. 113, no. 2, pp. 945-960, 2020.
[41]. Pandya, S., Shah, J., Joshi, N., Ghayvat, H., Mukhopadhyay, S.C. and Yap, M.H., 2016, November. A novel hybrid based recommendation system based on clustering and association mining. In Sensing Technology (ICST), 2016 10th International Conference on (pp. 1-6). IEEE.
[42]. Dr. Laxmi Lidiya. S. Suman, Rajest, "Correlative Study and Analysis for Hidden Patterns in Text Analytics Unstructured Data using Supervised and Unsupervised Learning techniques" in International Journal of Cloud Computing, International Journal of Cloud Computing (IJCC), Vol. 9, No. 2/3, 2020.
[43]. Rajasekaran R., Rasool F., Srivastava S., Masih J., Rajest S.S. (2020) Heat Maps for Human Group Activity in Academic Blocks. In: Haldorai A., Ramu A., Khan S. (eds) Business Intelligence for Enterprise Internet of Things. EAI/Springer Innovations in Communication and Computing. Springer, Cham
[44]. R. Regin, S. Suman Rajest and Bhopendra Singh, "Spatial Data Mining Methods Databases and Statistics Point of Views", Innovations in Information and Communication Technology Series, pp. 103-109, 28 February, 2021.
[45]. Shah, J., Pandya, S., N. Joshi, K. Kotecha, D. B. Choksi, Load Balancing in Cloud Computing: Methodological Survey on Different Types of Load Balancing Algorithms‖, IEEE International Conference on Trends in Electronis and Informatics, Tamilnadu, India, May 2017.
[46]. S. S Rajest Dr. Bhopendra Singh, P. Kavitha, R. Regin, Dr.K. Praghash, S. Sujatha, "Optimized Node Clustering based on Received Signal Strength with Particle Ordered-filter Routing Used in VANET" Webology, Vol.17, No.2, pp. 262-277, 2020.
[47]. Pandya, S., Vyas, D. and Bhatt, D., A Survey on Various Machine Learning Techniques‖, International Conference on Emerging trends in Scientific Research (ICETSR-2015), ISBN no: 978-81-92346-0-5, 2015.
[48]. Pandya, S., Wandra, K., Shah, J., A Hybrid Based Recommendation System to overcome the problem of sparcity‖, International Conference on emerging trends in scientific research, December, 2015.
[49]. Mehta, P., Pandya, S., A review on sentiment analysis methodologies, practices and applications, International Journal of Scientific and Technology Research, 2020, 9(2), pp. 601–609